Improvements to Pullout Failure Estimation in MSE Walls

Lalinda Weerasekara
WSP Canada, Vancouver, BC, Canada

ABSTRACT
The current practice of estimating the internal stability of Mechanically Stabilized Earth (MSE) structures entails use of empirical or semi-empirical methods to estimate the maximum reinforcement loads, which in turn is used to assess three potential failure modes, namely: (a) tensile rupture, (b) pullout and (c) connection failure of the reinforcement. These computations are performed at each reinforcement level, and the failure of the entire wall is assumed if the demand in at least one reinforcement exceeds the capacity of that failure mode. This paper discusses the limitations of assuming that the weakest reinforcement governs the stability of the entire reinforced soil mass, particularly in relation to displacement controlled failure mechanisms such as pullout. Other limitations of the current practice in estimating the pullout resistance are also discussed. To overcome these limitation, the Soil Reinforcement Interaction method (Weerasekara et al. 2017) is introduced, which explicitly accounts for the interaction between the reinforcement and backfill using a non-empirical analytical model. The method allows to compute a factor of safety for the entire reinforced soil mass and not only at each reinforcement level similar to the traditional practice. To further demonstrate the limitations of the existing methods and capabilities of the proposed method, two full-scale instrumented walls reinforced with smooth steel strips and high-strength nylon strips are discussed.

RÉSUMÉ
La pratique actuelle d'estimation de la stabilité interne des structures mécaniquement stabilisées (MSE) implique l'utilisation de méthodes empiriques ou semi-empiriques pour estimer les charges maximales de renforcement, qui à leur tour sont utilisées pour évaluer trois modes de défaillance potentiels, à savoir: rupture, (b) arrachement et (c) rupture de connexion du renforcement. Ces calculs sont effectués à chaque niveau de renforcement, et la rupture de toute la paroi est supposée si la demande dans au moins une armature dépasse la capacité de ce mode de défaillance. Cet article examine les limites de l'hypothèse selon laquelle le renforcement le plus faible gouverne la stabilité de l'ensemble de la masse du sol renforcée, en particulier par rapport aux mécanismes de défaillance contrôlés par le déplacement tels que le retrait. D'autres limitations de la pratique actuelle dans l'estimation de la résistance au retrait sont également discutées. Pour surmonter ces limitations, la méthode d'interaction entre le sol et le renforcement (Weerasekara et al., 2017) est introduite, ce qui explique explicitement l'interaction entre le renforcement et le remblai en utilisant un modèle analytique non empirique. La méthode permet de calculer un facteur de sécurité pour l'ensemble de la masse de sol renforcée et pas seulement à chaque niveau de renforcement similaire à la pratique traditionnelle. Afin de démontrer davantage les limites des méthodes et capacités existantes de la méthode proposée, deux murs instrumentés à pleine échelle renforcés de bandes d'acier lisses et de bandes de nylon à haute résistance sont discutés.

1 INTRODUCTION

The internal stability of Mechanically Stabilized Earth (MSE) walls is traditionally estimated by considering three potential modes of failures: (a) tensile rupture (b) connection failure and (c) pullout of reinforcement. The estimation of the tensile rupture of the reinforcement is relatively straightforward as considerable number of studies have been completed to develop methods to estimate the maximum reinforcement load at working stress conditions, using a variant of the following tributary area based method.

$$P_{max} = K\,\sigma'_v\,S_v S_h \qquad [1]$$

Where σ'_v is the vertical effective stress at reinforcement level, S_v and S_h are the vertical and horizontal spacing between reinforcements. K is an empirical lateral earth pressure coefficient which is selected to match the observations from pullout tests or instrumented walls, or alternatively assumed equal to the lateral earth pressure coefficient calculated from the classical earth pressure theories. In these methods, distinctly different K values are proposed for extensible and inextensible reinforcements with the intent of simulating the differences in reinforcement stiffness and soil-reinforcement interactions.

Without explicit account of soil-reinforcement interaction, the existing methods lack the ability to estimate the distribution of loads along the reinforcement - thereby the ability to estimate the load at the facing connection and pullout resistance. Faced with this limitation, the connection load is assumed similar to the predicted maximum reinforcement load (P_{max}) – although such assumptions contradict the actual measurements from instrumented test walls and basic mechanics related to friction development. Although the limitations in estimating the connection load is indisputable and well-known, most practitioners do not recognize the limitations in estimating the pullout resistance and its impact on the ultimate load carrying capacity.

The paper further discusses the limitations in the current approach of assuming that overall stability of the wall is related to the performance of the weakest link, especially in relation to pullout. At present, factor of safety is calculated at each reinforcement level and failure of one reinforcement in one of these failure modes is assumed to lead to the failure of the entire wall. To highlight the limitations of the existing methods, primarily relating to the ultimate failure state and pullout resistance estimations, results of two full-scale walls constructed using smooth steel strips and high-strength nylon strips are discussed in this paper.

2 PULLOUT RESISTANCE ESTIMATION

An inextensible reinforcement such as a steel strip reinforcement buried at a low overburden stress would experience virtually no elongation, thus it is generally expected that friction will be mobilized along the entire reinforcement length when subject to a small displacement. In essence, the displacement at the pulling end of the reinforcement is nearly equal to the displacement at the backend. In contrast, polymer reinforcements may experience considerable elongation before fully mobilizing the reinforcement length. Once the friction is fully mobilized over the entire reinforcement length, the trailing end displacement will be equal to the front-end displacement. The above behavior is largely governed by the reinforcement stiffness which is a key parameter influencing the soil-reinforcement interaction. With the exception of a few of methods, the reinforcement stiffness is not explicitly considered in the current design approaches.

The method for determining the reinforcement pullout resistance was originally proposed in the FHWA manual FHWA-RD-89-043 (Christopher et al., 1990), and has been the current state-of-practice with little or no modifications. The pullout resistance is related to the length of the reinforcement extending beyond the assumed failure surface and friction resistance acting on this reinforcement length. Once P_{max} is determined, the anchoring reinforcement length (L_e) required to resist this force is determined using the following semi-empirical relationship:

$$l_e = \frac{P_{max}}{F^* \alpha \sigma_v C R_c} \quad [2]$$

where C is a factor that accounts for the reinforcement surface area, R_c is the reinforcement coverage ratio, α is a scale effect correction factor and F^* is the pullout resistance factor. With the exception of α and F^* parameters, the remaining input parameters in this equation can be directly measured as they related to properties of reinforcement and soil. As a result, the approach predominantly relies on α and F^* parameters to account for the soil-reinforcement interaction and extensibility of reinforcement. In particular, parameter α is expected to represent the nonlinearity of the load – displacement which primarily depends on the extensibility of the reinforcement. In the absence of test data, Berg et al (2009) recommended α of 0.6 for geotextiles, 0.8 for geogrids and 1.0 for inextensible reinforcements. As demonstrated in this paper, the soil-reinforcement interaction is more complex than that expressed using these empirical factors.

Recognizing the importance of α and F^* on the overall pullout resistance computation, it is important to know how these parameters are determined. According to Berg et al (2009), pullout tests shall be performed on samples with a minimum embedded length of 600 mm. For inextensible reinforcements, the pullout resistance is the greater of the peak pullout resistance value prior to, or the value achieved at, a maximum leading end displacement of 20 mm. The above deflection limit was selected to limit the structure deformations in walls. For extensible reinforcements, the front-end displacement of 15 mm is recommended, and the intent was to establish the incipient of pullout instead of establishing a serviceability criteria. It is unclear how a unique front-end displacement of 15 mm relates to the pullout occurrence. The pullout test results indicate that mobilized length corresponding to a particular displacement level will depend on the overburden stress, reinforcement stiffness and soil characteristics. According to the above approach, multiple pullout test are required as there is no assurance that α and F^* values estimated at a particular overburden stress would represent the pullout resistance at other overburden stresses. It is impractical and uneconomical to conduct pullout tests at every overburden stress that reinforcement layers may encounter. In contrast, a framework that captures the basic mechanics of soil-reinforcement interaction would able to predict such pullout behaviors, thus require a fewer tests to determine the necessary parameters to model the entire wall.

In the current practice, the design lateral earth pressure distribution is pre-determined based on the perceived extensibility. For such computations, the reinforcements are classified as extensible or inextensible based on the material type in contrast to the actual elongation experienced by the reinforcement. For example, a polymer reinforcement with a higher axial stiffness (i.e., larger cross sectional area), located at a shallow depth may behaves as an inextensible reinforcement as the interface friction forces are not sufficient to develop significant elongation of the reinforcement. In contrast, a steel reinforcement of relatively smaller axial stiffness, located at depth may experience significant strain. Even if the same reinforcement is used in every layer, reinforcements at different depths will experience different reinforcement strains as such both extensible and inextensible reinforcements may coexist in a given wall. The extensibility (or strain) also depends on the reinforcement length on either side of the failure plane. As demonstrated in pullout tests, a reinforcement with a shorter embedded length will develop only a smaller strain irrespective of its material type. For the purpose of classifying the reinforcements based on the extensibility, some attempts have made to classify reinforcement extensibility using the soil stiffness as a reference. However, the above discussion indicates the limitations of using such approaches where extensibility depends on many other factors, not necessarily on the soil stiffness. British Standards (BS8006) recommends using the tie-back wedge method for walls with reinforcement strains greater

than 1% and coherent gravity method for strains below this limit. It is unclear how a unique value of 1% is selected as the demarcation for significantly different lateral earth pressure distributions. Furthermore, all reinforcement layers in a wall may not exceed or less than the threshold strain of 1% at all stages of loading. Alternative to the above approaches, Weerasekara et al. (2017) has shown that the behaviors of extensible and inextensible reinforcements are fundamentally similar thus there is no requirement to adopt different design parameters if the soil-reinforcement interaction is properly accounted. Importantly, the normalized lateral earth pressure distributions observed from instrumented walls can be analytically explained without the need for empirical correlations for earth pressure distribution that relies on the inferred reinforcement extensibility.

Irrespective of the limitations associated with the estimation of pullout resistance and connection loads, there are other key concerns related to the approach in which the ultimate limit state or the overall factor of safety is determined for the entire reinforced soil mass. Particularly in the current approach, computations are performed for each reinforcement level and the failure of the entire reinforced wall is assumed if the demand in one or more reinforcement exceeds its capacity. Nonetheless, it is unclear if failure of one reinforcement would lead to the failure of the entire reinforced soil mass, specifically if the failure is governed by a displacement-controlled failure mechanism such as pullout. Usually, such failure mechanism would engage a soil wedge that intersect several reinforcement layers.

Although most methods are capable of predicting the maximum reinforcement loads under working stress conditions with reasonable accuracy, our understanding of the ultimate collapse limit state is scarce. This is partly due to the limited number of full-scale instrumented test walls that can be used to validate the design approaches. The ability to predict the performance at working stress conditions is only part of the design challenge. Without the ability to validate the predictions for ultimate load carrying capacity, estimated factor of safety is not considered reliable. Based on the review of several case histories in which truncated base or reduced reinforcement lengths are utilized, Wu and Ooi (2015) stated that the current practice of estimating factor of safety against pullout is unrealistically conservative. Wu and Ooi (2015) also cited several case histories in which reinforcement lengths that ranged from 0.19 to 0.48 times the wall height (e.g., Segrestin 1994; Tatsuoka et al. 1997) have been successfully utilized. These lengths are much shorter than the minimum reinforcement length recommended in the current practice (i.e., 0.6 to 0.7 times wall height). In addition to the above, experiments have been performed where reinforcements were severed at certain locations such that anchoring length is gradually shortened until large wall deformations are observed (e.g., John 1985; Ketchart and Wu 1997). According to Wu and Ooi (2015), the current methods would have predicted the failure of these walls at a much earlier stage, highlighting the limitations in the current state-of-practice.

3 SOIL REINFORCEMENT INTERACTION MODEL

To overcome the above limitations, Weerasekara et al (2017) proposed a method called the Soil-Reinforcement Interaction (SRI) method, which forms an analytical framework for relating the reinforcement displacement, strain (or force) and mobilized friction length. The capabilities of this method in predicting wall performances under ultimate and working stress conditions are demonstrated in this paper and in the companion paper (i.e., Weerasekara, 2018). The details of the SRI method is given in Weerasekara et al (2017), therefore only a brief discussion is presented herein. In essence, the SRI method consists three sub-models:

(a) SRI Friction Model – Accounts for the soil-reinforcement interface friction;
(b) SRI Local Model – Accounts for the soil-reinforcement interaction in each reinforcement layer;
(c) SRI Global Model - Accounts for the equilibrium and interaction of multiple reinforcements in a reinforced soil mass.

3.1 SRI Friction Model

For the purpose of deriving a simplified analytical solution, the interface frictional behavior between soil-reinforcement is represented in a simplified form as shown in Figure 1. In this friction model, the maximum friction acting on the reinforcement per unit length (T_1) can be derived using the following equation:

$$T_1 = \frac{2bH\gamma \tan \varphi'_g}{1-[2(1+\upsilon)/((1-2\upsilon)(1+2K_0))] \tan \varphi'_g \tan \psi_{max}} \quad [3]$$

$$\psi_{max} = 6.25(I_D(Q - ln\sigma') - R) \quad [4]$$

where b is the width of the reinforcement, H is the burial depth, γ is the unit weight of the soil overburden, φ'_g is the soil-reinforcement interface friction angle, υ is the Poisson's ratio of soil, ψ_{max} is peak angle of dilation and K_0 is the "at-rest" lateral earth pressure coefficient estimated from the Jaky (1944) equation.

The proposed interface friction model accounts for the increase in friction due to constrained soil dilation at small displacements and gradual decrease in friction as the relative displacement between reinforcement and soil increases. These are important considerations especially for extensible reinforcements because different sections of the reinforcement will experience different magnitudes of friction due to the progressive development of friction along the reinforcement. As the magnitude of soil dilation also depends on the mean effective stress, Bolton (1986) classical stress-dilatancy framework was introduced to express the dilation in terms of relative density (I_D) and mean effective stress σ'. The parameters Q and R are constants that depend on the soil type. In the absence of specific tests to determine these parameters, Q and R were selected as 9 and 1, respectively for the two tests

discussed in this paper. According to this model, the additional frictional resistance developed from soil dilation is expected to decrease gradually and becomes negligible at a displacement of ($\overline{u_2}$). At this displacement, the interface friction per unit length (T_2) is given by the following:

$$T_2 = 2bH\gamma \tan \varphi'_g \quad [4]$$

The value of $\overline{u_2}$ is typically obtained from experimental observations, and considered as 150 times d_{50} after reviewing the experimental results published by Scarpelli and Wood (1982), Stone and Muir Wood (1992) and Vardoulakis et al. (1981). Typically, the results are relatively insensitive to the value selected for $\overline{u_2}$.

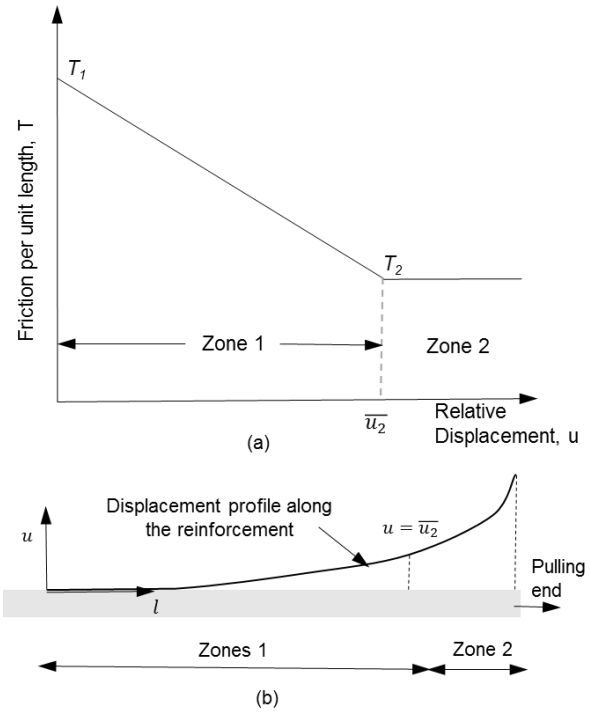

Figure 1. Schematic representation of the SRI Friction model

3.2 SRI Local Model

Once the interface frictional behavior is known, the SRI Local model is used to determine the interaction between reinforcement and soil by combining the SRI Friction model with the reinforcement stiffness. This is achieved by considering the equilibrium at an element level, which results in a second-order differential equation. The integration and substitution of boundary conditions lead to the SRI Local model that yields the following relationships for relative displacement (u), reinforcement strain (ε) and the mobilized frictional length along a reinforcement (l):

$$u = \left(\frac{\kappa}{\lambda}\right)\left(1 - \cos\sqrt{\lambda}l\right) \quad [5]$$

$$\varepsilon = \left(\frac{\kappa}{\sqrt{\lambda}}\right)\left(\sin\sqrt{\lambda}l\right) \quad [6]$$

$$l = \left(\frac{1}{\sqrt{\lambda}}\right)\cos^{-1}\left(1 - \frac{u\lambda}{\kappa}\right) \quad [7]$$

Where, $\lambda = \frac{(T_1 - T_2)}{J_r \overline{u_2}}$ and $\kappa = \frac{T_1}{J_r}$ and $\sqrt{\lambda}l < \frac{\pi}{2}$. The reinforcement load at any given location can be obtained as follows:

$$P = J_r \times \varepsilon \quad [8]$$

J_r is the stiffness of the reinforcement which is equal to the reinforcement modulus multiplied by the cross sectional area. Typically for geogrids, J_r is obtained from standard wide-width tensile tests (ASTM, 2001) and given per unit width with units of kN/m. As a simplification, the analytical model assumes a linear stress-strain relationship for the reinforcement (i.e., constant J_r), although certain polymer reinforcements at higher strain levels tends to exhibit nonlinear stress-strain response. Weerasekara and Wijewickreme (2010) developed a more detailed model to account for the nonlinearity and rate dependence of polymeric materials. However, for the purpose of simplifying the implementation of the SRI Local model for MSE walls constant J_r was considered.

The above equations form the framework to relate displacement, strain, force and mobilized frictional length along the reinforcement. Knowing any single parameter, the remaining parameters can be estimated. It is important to remind that T acts on the reinforcement as an external frictional force, whereas P is the force developed in the reinforcement due to this external frictional force. As a result, T is independent of the reinforcement stiffness, whereas P depends on the reinforcement stiffness. The SRI Local model was validated by modeling pullout tests and further details were provided in Weerasekara et al (2017).

3.3 SRI Global Model

Once the soil-reinforcement interaction occurring at each reinforcement level is known from the SRI Local model, the SRI Global model is used to assess the stability of the entire MSE wall. In essence, the method estimates the equilibrium by considering the driving forces/moments from lateral earth pressures and resisting forces/moments from reinforcement layers for different levels of wall displacements. The wall is in equilibrium when the driving and resistance forces/moments are equal. Besides the force equilibrium, the displacement compatibility is ensured as the method relies on the SRI Local method and appropriate boundary conditions. For estimating the lateral earth pressures, as a simplification, the Rankine theory was used to estimate the horizontal earth pressures and the slope of failure plane. The plane strain friction angle is used in these calculations, which is consistent with the expected failure mechanism.

In compliant with the recommendations given in the Canadian Standards Association (2014) and other research publications, the displacement required to

mobilize the active earth pressure condition was assumed 0.001 times the wall height for translational movements and 0.002 times the wall height for rotational movements. Furthermore, the at-rest lateral earth pressure is assumed to decrease linearly until the active earth pressure is fully mobilized at these threshold displacements. Alternatively, a more complex and non-linear relationship can be considered by the user. If applicable, compaction induced lateral earth pressures could also be included in the driving moment estimation. As the wall displacement increases from at-rest condition, the driving moment about the wall base is expected to decrease. Concurrently, the resisting moment is expected to increase with the wall displacement/rotation until tensile rupture or pullout of reinforcement occurs. MSE wall will be in equilibrium when the resisting moment is equal to the driving moment. The difference between horizontal driving forces and summation of reinforcement loads is the load developed at the toe (i.e., toe resistance).

A key aspect of the implementation of the SRI Global model is the proper application of the boundary conditions encountered in MSE walls. As schematically shown in Figure 2, any reinforcement can be classified into the following four categories based on the boundary conditions:

- No impact from boundary conditions (Case 1): The mobilized length measured from the failure surface is less than the distance to the wall facing or to the free end, therefore the equations derived from the SRI Local model are directly applicable without modifications.

- Free end of the reinforcement is mobilized (Case 2): In this case, the maximum tensile force is obtained using the SRI Local model with $l = L_2$ ($< L_1$). L_2 is the distance from the failure surface to the free end and L_1 is the distance from the facing to the failure surface. If the entire free length is mobilized, additional increase in displacement would not result in further increase in reinforcement load. This boundary condition is expected in relatively rigid reinforcements and at shallow burial depths, and directly related to the pullout failure mechanism. In other words, the factor of safety against pullout is equal to unity for that specific reinforcement.

- Load is developed at the wall facing (Case 3): The force in the reinforcement can be estimated using the SRI Local model until the mobilized length is equal to L_1 ($< L_2$). In a pullout test, once the entire reinforcement length is mobilized, the incremental displacements at the trailing and frontend will be similar (Δu). If one end is fixed (e.g., wall facing), the incremental increase in reinforcement force (ΔP) can be estimated using the following:

$$\Delta P = J_r \left[\frac{\Delta u}{L_1}\right] \qquad [9]$$

  ΔP is the load developed at the facing connection. If the wall facing is not fully rigid, a smaller connection load will be developed at the connection which depends on the rigidity of the wall facing. The total reinforcement force along L_1 length is the summation of ΔP and the reinforcement load (P) estimated from the SRI Local model.

- Load is developed at the wall facing and also the free length (Case 4): Initially the wall facing resistance is mobilized similar to Case 3, but further increase in displacement will mobilize L_2 length. When this occurs, tensile force in the reinforcement will not increase any further, similar to the Case 2.

In the following section, two full-scale walls are selected to demonstrate the limitations of the current approaches in estimating the pullout failures and also to demonstrate the capabilities of the SRI method. Both full-scale instrumented walls were constructed in 1976 at the U.S. Army Engineer Waterways Experiment Station (WES) and details are given in Al-Hussaini and Perry (1978). The first wall was reinforced with smooth steel strips while the other wall was reinforced with nylon strips. With the exception of reinforcement type and horizontal reinforcement spacing, the two walls were identical with respect to their final design height, vertical reinforcement spacing, reinforcement length, soil type and compaction effort. The existing design methods would predict these two walls to fail in pullout once they are at or near the design wall height because the estimated factor of safety against pullout is less than unity in the upper reinforcements. However, only the nylon strip wall failed due to pullout while the steel strip wall showed no signs of failure.

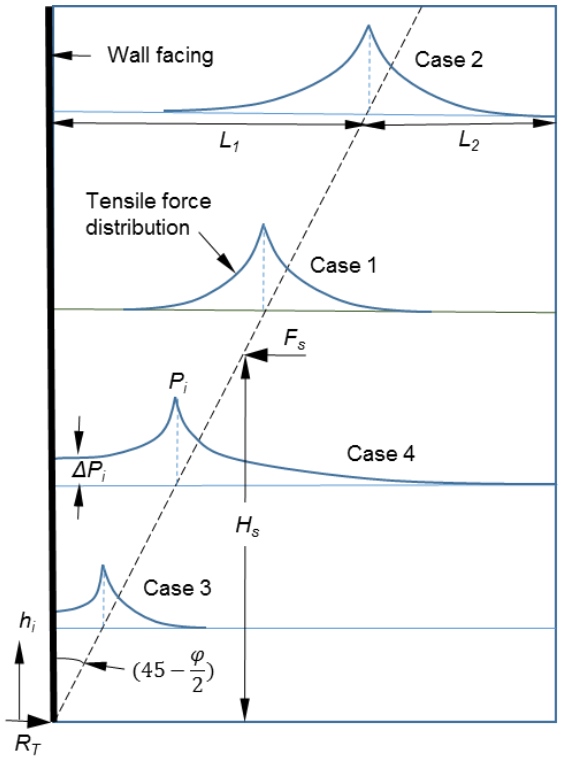

Figure 2. Forces acting on the MSE wall and different boundary conditions experienced by reinforcements.

3.4 Steel Strip Reinforced Wall

To the best of author's knowledge, this is the only full-scale instrumented wall with inextensible reinforcement that is surcharged to failure such that the ultimate load carrying capacity can be estimated. The wall was 3.66 m high, 4.9 m long and 3.1 m wide, and was constructed in a three-sided pit excavated at the test site. The wall was reinforced with six layers of smooth galvanized steel strips of 0.635 mm thick, 102 mm wide, 3.1 m long and with a spacing of 0.77 m horizontally and 0.6 m vertically. A yield strength of 352 MPa and an initial modulus of 214.6 GPa were measured from the uniaxial tensile tests conducted on steel strips. The ultimate strength was estimated to be about 430 MPa based on these experimental results. The wall facing consisted of high strength aluminum panels. The steel strips were connected to aluminum facings using double angle connectors and two bolts of 6.35 mm diameter. At the connection, the ultimate tensile strength was estimated to be about 24.5 kN/m, which was about 85% of the remaining section. The strains in the reinforcement were measured using series of strain gauges installed in the first, third and fifth layers from the bottom.

The wall was backfilled with clean sub-angular to angular concrete sand with a d_{50} of 0.48 mm. Direct shear tests conducted on the backfill soil yielded a peak friction angle of 36 degrees, which is equivalent to a plane strain friction angle of 41.1 degrees based on the empirical relationship proposed by Bolton (1986). Using a modified shear box, the interface friction angle between sand and smooth steel strips was measured to be 18 degrees. The dry unit weight of sand measured in the direct shear tests was 16.1 kN/m^3. During construction of the wall, the backfill was placed in 0.31 m lifts but was not compacted, therefore the additional horizontal stresses from compaction were not considered.

As stated previously, the wall did not fail due to pullout once it reached the design height. As the wall showed no signs of failure, the wall was surcharged to failure in increments of 12 kPa. The wall collapsed when the loading was in progress with an estimated surcharge load of approximately 90.4 kPa. The inspections of the collapsed wall have revealed that all failures occurred near the facing connection. The performance of the wall under all surcharge increments can be modeled using the SRI model by applying the surcharges and incrementally increasing wall deformation until the driving moment is equal to the resisting moment for all stage of loading. The SRI model shows that the required toe resistance (R_T) to maintain fixed conditions at the base is small for all surcharge increments (i.e., less than 4 kN/m). Therefore, the wall is likely to rotate about its base, which is consistent with the measured wall deformation pattern. The key input parameters used in the SRI model are summarized in Table 1. Figure 3(a) and (b) show the resisting and driving moments calculated prior to surcharging and with a surcharge of 90 kPa. Other surcharge increments are not shown for brevity.

Table 1. Key input parameters for the SRI model

Wall	φ'_g(deg)	J_r(kN/m)
Smooth Steel Strip	18	17980
Nylon Strips	30	70

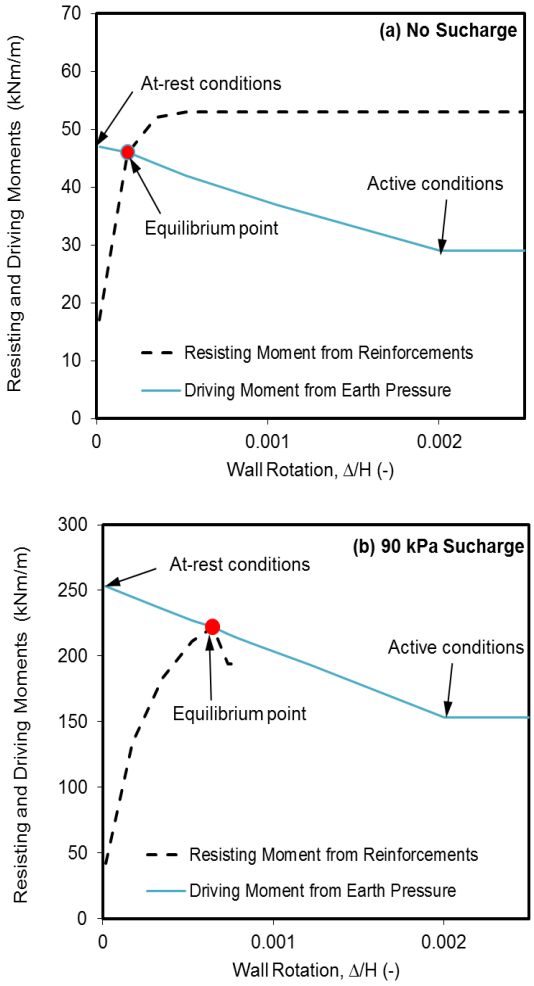

Figure 3. Resisting and driving moments calculated (a) prior to surcharging and (b) with a surcharge of 90 kPa for steel strip reinforced WES wall.

For each loading condition, equilibrium is achieved when the driving moment is equal to the resisting moment from reinforcements. According to the SRI model, at a surcharge of 90 kPa, the failure was imminent as the connection load in the bottom three layers have approached the tensile strength limit of 24.5 kN. When this threshold load is exceeded, the tensile rupture was simulated by setting the connection strength to zero.

It is important to recognize that the SRI method is capable of estimating the load distributions along each reinforcement, whereas other design methods are only capable of estimating the maximum reinforcement load. For example, Figure 4 shows the measured and estimated

strain distributions from the SRI method prior to surcharging.

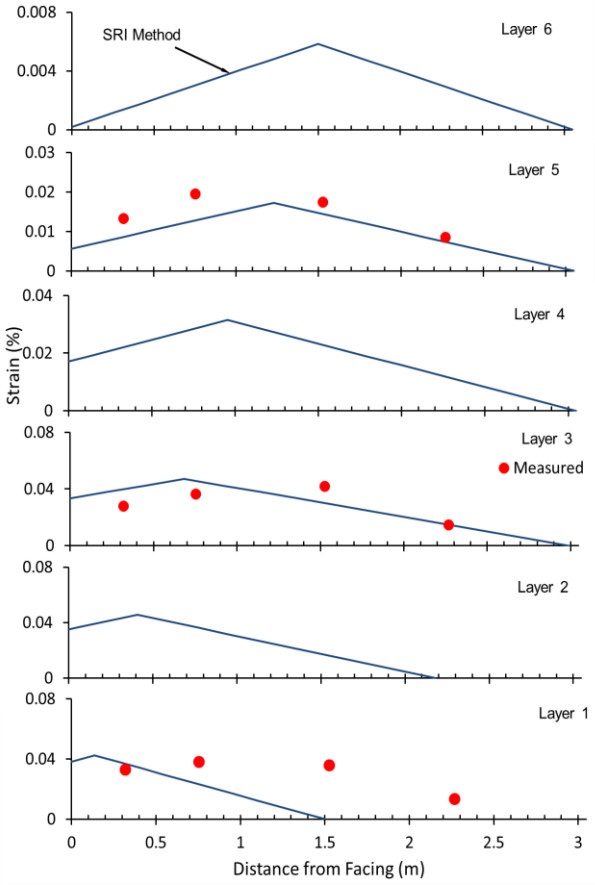

Figure 4. Measured and estimated strain distributions along reinforcements before surcharging (steel strip reinforced WES wall).

3.5 Nylon Strip Reinforced Wall

The second instrumented wall is a rare occurrence where the wall failure is clearly attributed to pullout. The wall was reinforced with heavy neoprene-coated nylon fabric strips of 100 mm wide, 2 mm thick and 3.05 m long. The tensile test performed on strips showed a constant modulus of 415 MPa up to a strain of 7%. Although details were not provided, Al-Hussaini and Perry (1978) reported an interface friction angle of 30 degrees from three direct shear tests. The horizontal spacing of reinforcements was 1.2 m, while the vertical spacing, backfill and construction technique were similar to the steel strip reinforced wall. As stated earlier, the wall failed due to pullout after reaching a height of 3.05 m. Figure 5 shows the resistance and demand curves obtained using the SRI method. Compared to the steel strip wall, relatively low reinforcement stiffness leads to a gradual development of resistance compared to the sharp increase in resistance observed in the steel strip reinforced wall. As a result, the nylon strip wall requires a larger displacement to reach equilibrium, which is greater than the displacement required to mobilize the full active soil resistance. This is interpreted as pullout failure of the reinforced soil mass. It is likely that the reported interface friction angle of 30 degrees may have been influenced by soil dilation, therefore the actual large-displacement interface friction angle required for the SRI method would have been smaller. If so, even larger displacement is required to reach equilibrium. These demand/resistance plots can be used to explain the relative ductile and brittle behaviors observed in structures reinforced with different reinforcement types.

The maximum reinforcement strain estimated using the SRI method is less than 4%, which is much smaller than the reported ultimate strain of 14.5%. The inspection of the failed wall did not indicate reinforcement rupture which is consistent with the estimations. Nonetheless, it is not possible to confirm the accuracy of strain estimates since reinforcement strains were not directly measured.

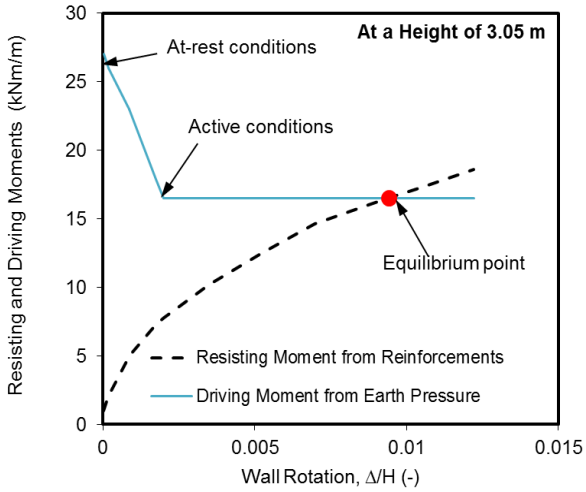

Figure 5. Resisting and driving moments calculated for the nylon strip reinforced WES wall at a wall height of 3.05 m.

4 DISCUSSION

4.1 Influence of Reinforcement Stiffness

Above two case histories demonstrate the importance of reinforcement stiffness and its influence on the failure mechanism. For example, in the absence reinforcement stiffness in the formulation, the existing methods such as the AASHTO Simplified method (AASHTO 2002) would predict pullout failures in both walls. In contrast, the SRI method correctly predicted the failure of the nylon strip reinforced wall, and most importantly the non-failure of the steel strip reinforced wall. Regardless of the differences in reinforcement stiffness, the SRI model demonstrates that the fundamental wall behavior to be similar in these two walls, especially if the soil-reinforcement interaction is considered. This is a vital conclusion since the method does not require to select different design parameters (e.g., lateral earth pressure coefficients) for different reinforcement types as recommended in the existing design methods. Instead, using the actual reinforcement

stiffness and interface friction angle, the behaviors of MSE walls with different reinforcement types can be estimated.

4.2 Improvements to Factor of Safety Calculations

Prior to surcharging of the steel strip reinforced wall, the existing design approaches will estimate a factor of safety less than unity against pullout in the upper reinforcement layers. For the same loading condition, the SRI method also predicts full mobilization of reinforcement length in the upper four reinforcement layers (see Figure 4). The maximum tensile force developed in the upper reinforcement layers are governed by the "Case 2" boundary condition, such that further increase in wall displacement would not increase the reinforcement load as the entire reinforcement length is already mobilized. This is expected as steel strips require only a small displacement to mobilize its entire reinforcement length due to its relatively high reinforcement stiffness in the axial direction – this is also analytically shown using the SRI Local model. Despite the full mobilization of friction along the reinforcement, the experimental results and SRI method demonstrate that mobilization of entire reinforcement length would not necessarily lead to failure. Although most of the reinforcement contribution is utilized, only a small fraction of the soil strength is developed when the equilibrium is reached. Therefore, the safety margin is largely provided by the soil resistance that has not been mobilized. For example, the estimated ultimate resisting moment using the SRI method is 53 kNm/m for the steel strip reinforced wall before surcharging. The ultimate driving moment occurs when the full soil strength is mobilized (i.e., active conditions) which is estimated to be 29 kN/m. Consequently, a factor of safety of about 1.83 is estimated for this wall at the end of construction, compared to a value less than unity predicted by other methods based on calculations performed for each reinforcement level. However, for walls with incremental facing panels, calculation checks should be performed for rotational or translational failures that could initiate from different reinforcement levels (i.e., not necessarily from the toe of the wall), and the design will be governed by the most critical failure mechanism.

With the above background, reinforcement load/strain distributions of other instrumented test walls can be examined to confirm if similar situations encountered at working stress conditions. Due to the prominence given to the maximum reinforcement load in the current design practice, most case histories show only the maximum tensile load and a few case histories show the distribution of strain/load along their reinforcements. Minnow Creek wall is one of the instrumented walls that shows the reinforcement load distributions, and readers are referred to Runser et al (2001) for more details. The reinforcement length was 15.4 m in the bottom four layers and 12 m in the remaining layers. The reinforcement load distributions indicate full mobilization of friction possibly in reinforcement layers located in the upper 12 m. The wall was designed for a minimum factor of safety of 1.5 against pullout for each reinforcement layer. However, the measured reinforcement strain distributions contradict this assertion as the estimated factor of safety is equal to unity against pullout in the upper reinforcements. As indicated by the wall deformations measured immediately after construction (only 30 mm for this 16.9 m high wall), the wall is not in danger of collapse from pullout and likely to have met the design intent.

Solely from an internal stability standpoint, the proposed analytical method shows the potential for using different reinforcement lengths for the purpose of optimizing the reinforcement usage, as opposed to the current approaches in which uniform reinforcement lengths are recommended irrespective of the actual design needs. In particular, the SRI method indicate that shorter reinforcement lengths would be sufficient near the base, provided that external stability requirements are satisfied especially in relation to sliding. Intuitively, longer reinforcements at the top would improve the stability of wall against tilting and pullout, and the SRI method provide a framework to quantify the contribution from these reinforcements and select appropriate reinforcements for these layers. In practice, this would be an important consideration if a hard surface is required to be excavated and removed to accommodate a uniform reinforcement length. Similar situations may occur when obstructions such as existing retaining walls are encountered near the wall base making it impossible to provide the minimum specified reinforcement length required to satisfy the factor of safety requirement for pullout.

Similarly, when the reinforcement length is limited by vertical or horizontal obstructions (e.g., manholes, utilities, culverts), the SRI method provide a rational framework to estimate the impact of this deficiency. As the overall factor of safety is not necessarily depends on the weakest reinforcement, the reduced contribution from a shorter reinforcement can be compensated by making changes to the remaining layers (i.e., using stiffer and/or longer reinforcements). Aforementioned discussion highlight the need to re-evaluate the minimum reinforcement length requirements. The minimum reinforcement length should account for the reinforcement stiffness which directly influences the mobilized friction length.

It is important to note that the SRI method allows to predict wall performances under various stages of loading, not only for the working stress conditions for which the existing methods are calibrated. Similarly, it is important to note that the SRI method does not require the distribution of the maximum reinforcement load to be pre-determined unlike other tributary area based methods. Weerasekara et al (2017) demonstrated that the shape of the maximum reinforcement load is likely to change when the load changes.

5 CONCLUSIONS

The paper demonstrates the advantages of the proposed approach for estimating the factor of safety for the entire reinforced soil mass against internal failure by considering the soil-reinforcement interaction and boundary conditions. This an alternative to the conventional approach of estimating factor of safety for each reinforcement layer without considering the development of a failure mechanism that could impact the entire reinforced soil

mass. Although factors of safety for each reinforcement level can be estimated using the SRI method, the two case histories discussed in this paper demonstrate the limitation of this approach. At working stress conditions, full-scale instrumented walls with inextensible reinforcements indicate that the actual factor of safety against pullout can be equal to unity in some reinforcements although the minimum targeted design factor of safety is 1.5 using the traditional design methods. Despite fully mobilizing the full contribution from reinforcements, the additional resistance against failure is provided by the soil resistance that has not been mobilized.

In the development of the SRI method, certain simplifications (e.g., linear variation of lateral earth pressure with wall displacement, constant stiffness for polymer reinforcements) were introduced with the intent of obtaining a more user-friendly analytical tool for day-to-day engineering applications. Even with these simplifications, the SRI method predictions remain reasonably accurate for engineering designs. Nevertheless, the reader may choose to replace these simplifying assumptions by incorporating more sophisticated models into the analytical framework presented in this paper. Spreadsheet and implementation guidelines for the SRI method will be upon request or can be downloaded through the supplementary data package provided along with Weerasekara et al. (2017).

ACKNOWLEDGEMENT

Author would like to acknowledge the funding support from his former employer, Tetra Tech through the Applied Technology and Development program.

REFERENCES

AASHTO. 2002. *Standard Specifications for Highway Bridges,* 17th Edition, American Association of State Highway and Transportation Officials, Washington, D.C.

Al-Hussaini, M. & Perry, E. B. 1978. Field Experiment of Reinforced Earth Wall. *Journal of Geotechnical Engineering Division*, ASCE, 104(3): 307–322.

ASTM 2001. Standard Test Method for Determining Tensile Properties of Geogrids by the Single or Multi-Rib Tensile Method (D6637), ASTM International, West Conshohocken, Pennsylvania.

Bolton. M. D. 1986. The Strength and Dilatancy of Sands. *Geotechnique*, 36(1): 65-78.

Canadian Standards Association. 2014. *Canadian Highway Bridge Design Code (CHBDC)*. CSA Standard S6-14, Canadian Standards Association, Toronto, Canada.

Christopher, B. R., Gill, S. A., Giroud, J.-P., Juran, I., Mitchell, J. K., Schlosser, F. & Dunnicliff, J. 1990. *Reinforced Soil Structures, Volume 1: Design and Construction Guidelines*. Federal Highway Administration (FHWA), Report No. FHWA-RD-89-043, Washington, D.C.

Berg, R.R; Christopher, B. R., & Samtani, N.C. 2009. *Design of Mechanically Stabilized Earth Walls and Reinforced Soil Slopes,* Federal Highway Administration (FHWA), Report No. FHWA-NHI-10-024, Washington, D.C.

Jaky, J. 1944. The Coefficient of Earth Pressure at Rest. *Journal of Society of Hungarian Architects and Engineers*, October: 355-358.

John, N.W.M. 1985. Collapse Test on a Reinforced Soil Wall, Failure in Earthworks, Thomas Telford Ltd., London.

Ketchart, K. and Wu, J.T.H. 1997. Performance of Geosynthetic-Reinforced Soil Bridge Pier and Abutment, Denver, Colorado, USA. *Special Presentation, International Symposium on Mechanically Stabilized Backfill*, A. A. Balkema Publishers, The Netherlands, 101-116.

Runser, D. J., Fox, P. J., and Bourdeau, P. L. 2001. Field Performance of a 17 m-high Reinforced Soil Retaining Wall. Geosynthetic International, 8(5): 367–391.

Scarpelli, G. & Wood, D. M. 1982. Experimental Observations of Shear Band Patterns in Direct Shear Tests. *Proceedings of IUTAM Conference on Deformation and Failure of Granular Materials*, 31st Aug to 3rd Sept, Delft.

Stone, K. J. L. & Muir Wood, D. 1992. Effects of Dilatancy and Particle Size Observed in Model Tests on Sands. *Soils and Foundations,* 32(4): 43-57.

Vardoulakis, I., Graf, B. & Gudehus, G. 1981. Trap-door Problem with Dry Sand: A Statistical Approach Based upon Model Test Kinematics. *International Journal for Numerical and Analytical Methods in Geomechanics*, 5(1): 57-78.

Weerasekara, L. 2018. Steel Strip Reinforced Walls under Working Stress Conditions, *GeoEdmonton*, 71st Canadian Geotechnical Conference, Edmonton, BC.

Weerasekara, L., Hall, B.E., & Wijewickreme. 2017. A New Approach for Estimating Internal Stability of Reinforced Soil Structures, *Geosynthetic International,* 24(4): 419 – 434.

Weerasekara, L. & Wijewickreme, D. 2010. An Analytical Method to Predict the Pullout Response of Geotextiles. *Geosynthetic International,* 17(4): 193-206.

Wu, J.T.H. and Ooi, P. S.K. 2015. Synthesis of Geosynthetic Reinforced Soil Design Topics, Federal Highway Administration (FHWA), Report No. FHWA-HRT-14-094, Washington, D.C.